J Solid State Electrochem (2016) 20:1303–1309
DOI 10.1007/s10008-016-3125-7

ORIGINAL PAPER

Coralloid and hierarchical Co_3O_4 nanostructures used as supercapacitors with good cycling stability

Xiuhua Wang[1,2] · **Xiaoxiu Wu**[1] · **Bingang Xu**[2] · **Tao Hua**[2]

Received: 24 September 2015 / Revised: 29 November 2015 / Accepted: 12 January 2016 / Published online: 21 January 2016

Abstract Coralloid and hierarchical Co_3O_4 nanostructures were synthesized by a facile two-step approach composed of room temperature solution-phase synthesis without any surfactant and calcination of precursor. Owing to the unique structural features, the capacitance of Co_3O_4 could reach up to 591 F g^{-1} at a current density of 0.5 A g^{-1}. Especially the cycling stability remained about 97 % after 2000 cycles at a current density of 1 A g^{-1}. These results demonstrated that the coralloid and hierarchical Co_3O_4 were excellent candidates for electrochemical supercapacitor devices.

Keywords $Co(OH)_2$ nanosheets · Coralloid Co_3O_4 · Supercapacitor · Solution-phase process · Hierarchical

Introduction

Nowadays, energy problems have become the greatest focus attracting the world's attention and triggering tremendous efforts for energy storage and conversion. To satisfy the growing energy costs, energy storage devices are demanded for high-power applications. Supercapacitors, also called electrochemical capacitors, are a new class of energy storage device and have great applications in electric vehicles and mobile electronics, owing to the high power density, long cycle life, short charging time, and environmental benignity [1–4].

According to the charge storage mechanism, supercapacitors can be divided into two categories, namely, electric double-layer capacitors (EDLC) and pseudocapacitors [5–7]. The research of pseudocapacitors based on metal oxides and hydroxides have received considerable attention over the past decades owing to their large capacitance and fast redox kinetics [8]. RuO_2 has excellent pseudocapacitive performance, but it is expensive and poisonous [9]. Therefore, efforts have been devoted to developing new supercapacitor electrode materials. Among these materials, Co_3O_4 could serve as alternative of the expensive RuO_2 because of its high theoretical specific capacitance (3560 F g^{-1}), environmentally benign nature, and lower cost [10–14].

Various Co_3O_4 nanostructures including one-dimensional (1D) nanowires, nanorods, nanotubes, nanoparticles, and nanosheet have been synthesized with the method of hydrothermal, solvothermal, electrospray deposition, coprecipitation, microemulsions, chemical vapor deposition, sol–gel methods, and so on [15–18]. Among the reported nanostructures, 1D Co_3O_4 shows better performance in energy storage owing to its fast electron transport and large active interfacial sites along the long dimension [19–21]. For example, Razeeb et al. designed Co_3O_4 nanowire hybrid structure on carbon fiber cloth via a facile hydrothermal approach followed by thermal treatment in air [22]. Xu group reported surfactant-dependent self-organization of Co_3O_4 nanowires on Ni foam for high-performance supercapacitors [23]. Li et Al. synthesized Co_3O_4 nanowires growing on the ZnO nanorods through

Electronic supplementary material The online version of this article (doi:10.1007/s10008-016-3125-7) contains supplementary material, which is available to authorized users.

✉ Xiuhua Wang
xhwang@mail.ahnu.edu.cn

✉ Bingang Xu
tcxubg@polyu.edu.hk

[1] The Key Laboratory of Functional Molecular Solids, Ministry of Education, College of Chemistry and Materials Science, Anhui Normal University, Wuhu 241000, China

[2] Nanotechnology Center, Institute of Textiles and Clothing, The Hong Kong Polytechnic University, Hung Hom, Kowloon, Hong Kong, People's Republic of China

hydrothermal method combined with annealing treatment [24]. Khan et al. reported the electrochemical properties of the 1D hybrid nanoarchitecture of Co_3O_4-NiO mixed oxide nanoshell grown on Co-Ni metal alloy core nanowires with the high capacitance of 2013 F g^{-1} at 2.5 A g^{-1} [25]. Wang et al. synthesized Co_3O_4 nanowires by a facile hydrothermal method, and the capacitance was 240 F g^{-1} at 1 A g^{-1} [26]. However, the pure coralloid and hierarchical Co_3O_4 nanostructures with good supercapacitor performance have rarely been reported.

Although 1D pure Co_3O_4 nanostructures have been obtained by the thermal annealing $Co(OH)_2$ precursors [27–29], there are still several challenges in the synthetic route and the performance. One is that some methods are quite intricate, are costly, and result in environment pollution, which is hard to realize in industrialization. The other challenge is the poor supercapacitor cycling stability. Therefore, it is urgently required to find a simple and low-cost route to realize the morphology control of Co_3O_4 nanostructures and to fabricate well-defined hierarchical Co_3O_4 nanostructure with high cycling stability.

Motivated by the above concerns, we report a successful attempt at the fabrication of coralloid and hierarchical Co_3O_4 nanostructures via a facile room temperature reprecipitation method and thermal treatment. The as-prepared coralloid and hierarchical Co_3O_4 nanomaterials exhibited good supercapacitor performance with high stability. It is expected that the simple and economical route to obtain Co_3O_4 nanostructure will greatly promote their industrial application.

Experimental

Synthesis of $Co(OH)_2$ nanosheets and coralloid and hierarchical Co_3O_4 nanostructures

The $Co(OH)_2$ nanosheets were synthesized by solution-phase process at room temperature. Solutions were prepared using 10 mL ethylene glycol and 10 mL methanol under the magnetic string, and then 0.2 g $Co(NO_3)_2{\cdot}6H_2O$ was dissolved in the mixed solution. After stirring to dissolve, 0.4 g NaOH was added into the above solution followed by an amount of molybdenum trioxide nanorods [30]. After stirring for 10 min, 2 mL 80 % hydrazine hydrate ($N_2H_4 \cdot H_2O$) was added dropwise. The mixed solution was stirred for another 30 min at room temperature, and the pink products were collected, rinsed several times with ethanol, and then dried in vacuum at 60 °C for 21 h. Finally, the coralloid and hierarchical Co_3O_4 nanostructures were obtained by calcining pink $Co(OH)_2$ nanosheets at 300 °C for 3 h in a muffle furnace in the air atmosphere.

Material characterization

X-ray powder diffraction (XRD) patterns were obtained on a Rigaku Max-2200 with Cu Ka radiation in the 2θ range of 10°–80°. The scanning electron microscopy (SEM) images were taken with a Hitachi S-4800 field emission scanning electron microscope. The transmission electron microscopy (TEM) images were recorded on a FEI Tecnai G^2 20 high-resolution transmission electron microscope performed at an acceleration voltage of 200 kV. The surface area of the as-obtained sample was computed from the results of N_2 physisorption at 77 K (model: BECKMANSA3100COULTER) using the Brunauer–Emmett–Teller (BET) formalism.

Electrochemical measurements

The capacitive performances of the as-prepared coralloid and hierarchical Co_3O_4 nanomaterials were measured on a CHI 660E electrochemical working station (ChenHua Corp., Shanghai, China) with a three-electrode experimental setup. The working electrode was made of the as-prepared Co_3O_4 (80 wt%), acetylene black (15 wt%), and polytetrafluoroethylene (PTFE) binder (5 wt%). And, a 3 M KOH aqueous solution was used as the electrolyte. After grind uniform, the mixture materials were pasted onto a piece of nickel foam and dried under vacuum at 60 °C for 3 h. Platinum wire and standard calomel electrode (SCE) were used as the counter and reference electrodes, respectively. The specific capacitance (C) of the electrode can be evaluated according to the following equation:

$$C = \frac{I \times \Delta t}{m \times \Delta V} \quad (1)$$

where C (F g^{-1}) is the specific capacitance of the electrode based on the mass of active materials, I (A) is the current during discharge process, Δt (s) is the discharge time, ΔV (V) is the potential window, and m (g) is the mass of active materials.

Results and discussion

Material characterization

Figure 1a displays the X-ray powder diffraction (XRD) patterns of the $Co(OH)_2$ precursor. It can be seen that all of the diffraction peaks can be perfectly indexed to monoclinic $Co(OH)_2$ (JCPDS No. 45-0031), and no excrescent peaks are detectable. The morphology of the as-prepared samples was studied by SEM and TEM. Figure 1b shows that the morphology of $Co(OH)_2$ is leaf-like sheets with lengths of about 3 μm and thickness of about 250 nm. Under a higher magnification (Fig. 1c), it can be observed that these leaf-like sheets consisted of very thin nanoflakes with thickness of about 10 nm, which are overlapping and connected with each other. The TEM investigation (Fig, 1d) further demonstrates that $Co(OH)_2$ nanosheets consisted of nanoflakes.

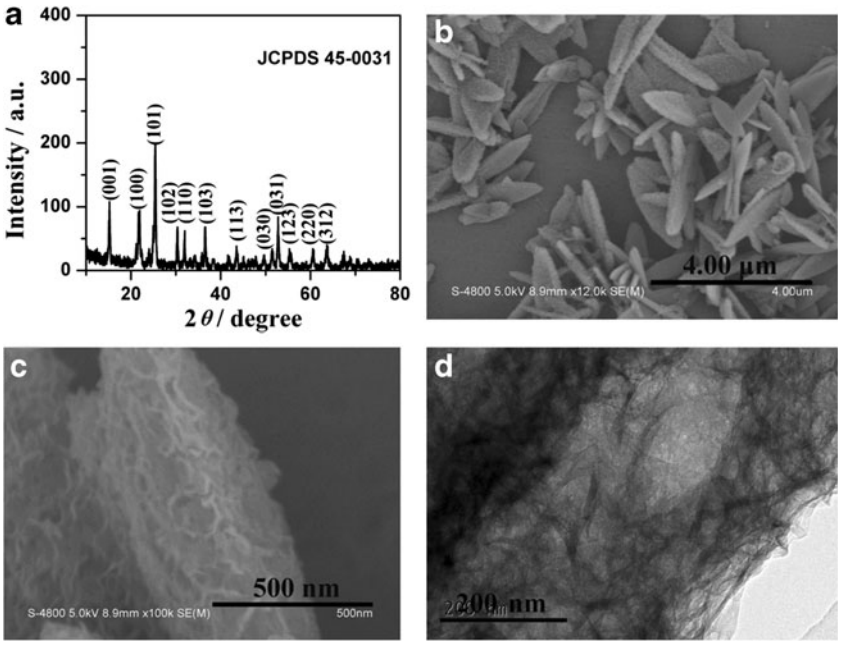

Fig. 1 **a** XRD pattern; **b** SEM image; **c** high-magnification SEM image; and **d** TEM image of the $Co(OH)_2$ crossed nanosheets

The XRD patterns of as-synthesized Co_3O_4 are shown in Fig. 2a. All the patterns can be assigned to the (1 1 1), (2 2 0), (3 1 1), (4 0 0), and (5 1 1) planes of Co_3O_4 (JCPDS No. 42-1467), respectively. The absence of the precursor peaks suggests that the precursor was completely transformed into Co_3O_4. Figure 2b shows that the morphology of the Co_3O_4 is coralloid. From the high-magnification image, we can see that the coralline branches are formed by close stacking of 30–50-nm nanoparticles, as shown in Fig. 2c. The TEM investigation further demonstrates that the morphology of Co_3O_4 is coralloid and hierarchical nanostructure, and the inset indicates the hierarchical structures of nanoparticles stacking on bundled nanorods, as shown in Fig. 2d.

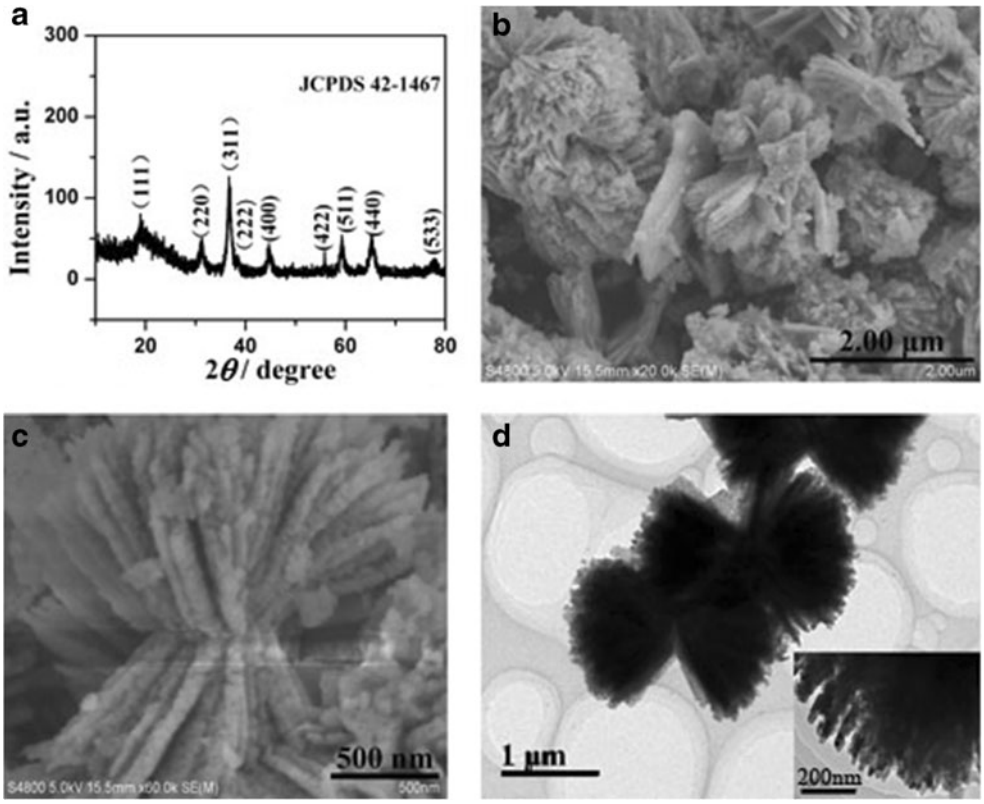

Fig. 2 **a** XRD pattern; **b** SEM image; **c** high-magnification SEM image; and **d** TEM image of the coralloid and hierarchical Co_3O_4 nanostructures, and the inset is the high-magnification image of TEM

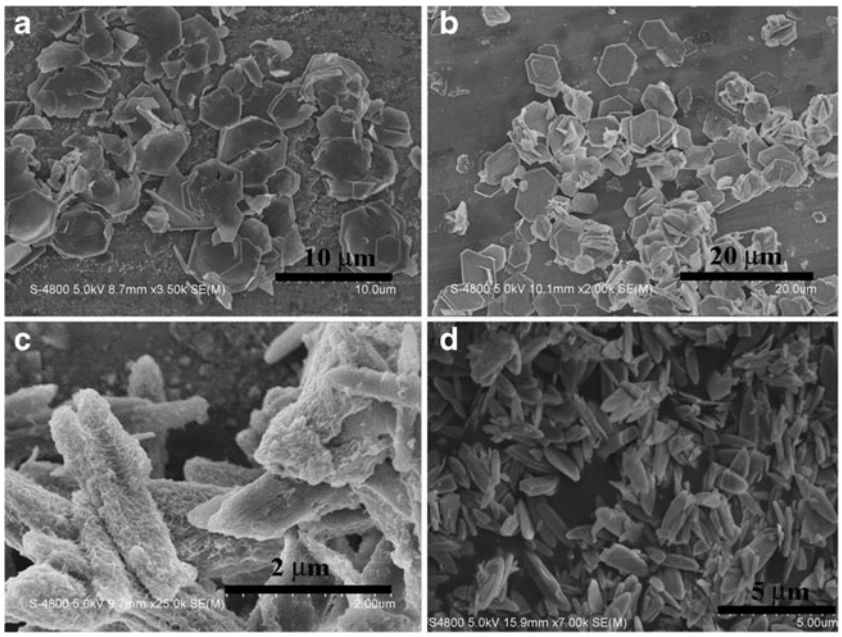

Fig. 3 SEM morphologies of the precursor $Co(OH)_2$ under the different reaction conditions: **a** without $N_2H_4{\cdot}H_2O$; **b** without the MoO_3 nanorods; **c** 10-min reacting time; **d** over 30-min reacting time

Growth mechanism

As well known, the morphology of the precursor $Co(OH)_2$ directly influences the morphology of Co_3O_4. In order to explore the formation mechanism of $Co(OH)_2$ nanoflakes, a series of conditional experiments were carried out and the intermediate products were characterized by SEM. Without the $N_2H_4{\cdot}H_2O$ reagent, the obtained morphology of the product is large and amorphous, as shown in Fig. 3a. Without the MoO_3 nanorod reagent, the obtained morphology of the product is large hexagonal-like platelet, as shown in Fig. 3b. There are also other factors that affect the morphology and uniformity of $Co(OH)_2$ nanostructures, such as the reacting time. Figure 3c shows that the morphology of the intermediate product prepared only for reacting 10 min. If the reacting time is over 30 min, the morphology of the product is aggregated plates, as shown in Fig. 3d. After the calcination of the as-prepared precursor, the coralloid and hierarchical Co_3O_4 nanostructures could only be obtained through $Co(OH)_2$ owned the crossed leaf-like nanostructures.

The following reactions may occur during the whole process [31–33]:

$$Co^{2+} + 2OH^- \rightarrow Co(OH)_2 \quad (2)$$

$$6Co(OH)_2 + O_2 \rightarrow 2Co_3O_4 + 6H_2O \quad (3)$$

On the basis of the above experimental results and analysis, the morphological evolution process of the coralloid and hierarchical Co_3O_4 nanostructure was presumed and illustrated in Scheme 1. At the initial stage, the $Co(OH)_2$ nuclei were formed from the precipitation reaction according to Eq. (2), as shown in Scheme 1a. Then, these nuclei began to grow and tended to assemble nanoflakes owing to high surface energies (Scheme 1b). $N_2H_4{\cdot}H_2O$ played an important role in the reaction, keeping the alkaline environment and preventing the product to oxidate. MoO_3 nanorods acted as soft template, which could be dissolved in $N_2H_4{\cdot}H_2O$. By the cooperation of $N_2H_4{\cdot}H_2O$ and MoO_3 nanorods, the nanoflakes aggregate into crossed leaf-like structures, as shown in Scheme 1c. At the second stage, $Co(OH)_2$ was decomposed into Co_3O_4 at high temperature of about 300 °C [Eq. (3)]. Accompanied by the release of CO_2 and H_2O gases during the precursor

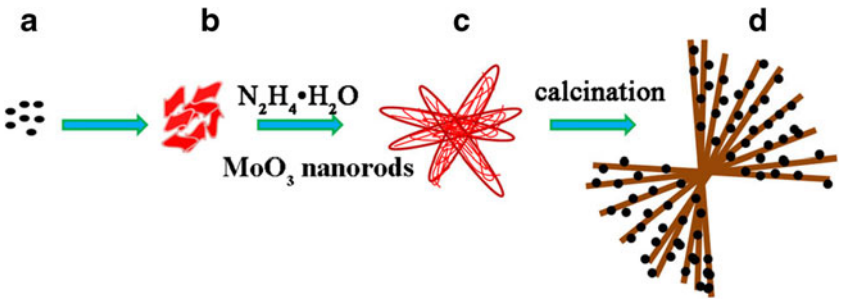

Scheme 1 Schematic illustration of the morphological evolution process of coralloid and hierarchical Co_3O_4 nanostructures: **a** $Co(OH)_2$ nuclei; **b** $Co(OH)_2$ nanoflakes; **c** $Co(OH)_2$ crossed sheets; **d** coralloid and hierarchical Co_3O_4 nanostructures

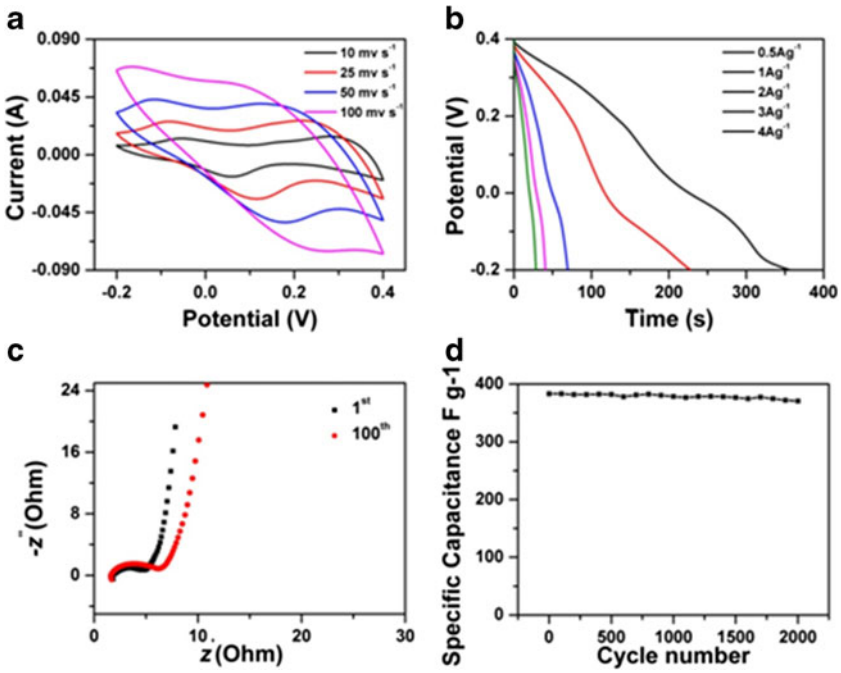

Fig. 4 **a** CV curves of coralloid and hierarchical Co_3O_4 nanomaterials at various scan rates in 3 M KOH; **b** charge–discharge curves at a series of current densities for as-obtained Co_3O_4 electrode in 3 M KOH; **c** the electrochemical impedance spectra of the electrodes at the first and 100th cycles; **d** long-term stability curves of Co_3O_4 electrodes at a current density of 1 A g^{-1}

calcination process, the internal nanoflakes would transform to the nanorods and the external nanoflakes would shrink to nanoparticles and aggregate together on the surface of the nanorods. Finally, coralloid and hierarchical Co_3O_4 nanostructures were obtained, as shown in Scheme 1d. Of course, it still needs more detailed and systematic work to provide evidence to make clear the precise growth mechanism of the coralloid and hierarchical Co_3O_4 nanostructures.

Electrochemical properties

The as-prepared coralloid and hierarchical Co_3O_4 nanostructures were fabricated into supercapacitor electrodes, and their supercapacitive behaviors were estimated by employing the cyclic voltammetry (CV), galvanostatic charge–discharge (GCD), electrical impedance spectroscopy (EIS), and the cycling stability measurements.

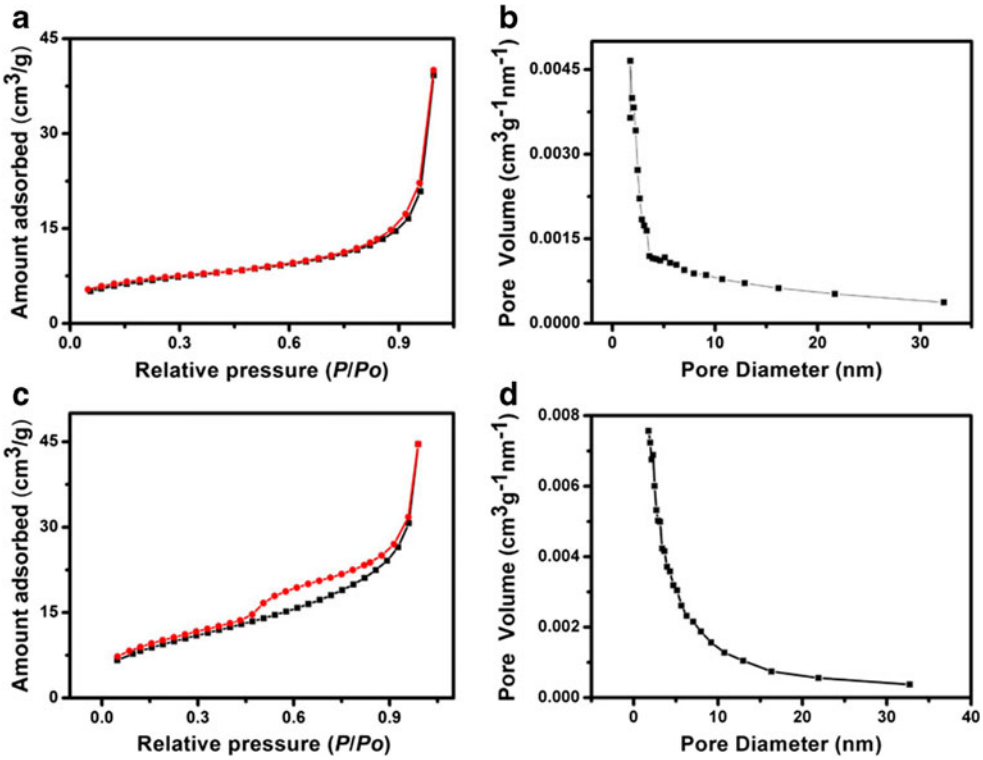

Fig. 5 BET spectra of the as-obtained **a** $Co(OH)_2$ crossed nanosheets and **c** coralloid and hierarchical Co_3O_4; and the BJH pore size distribution of **b** $Co(OH)_2$ leaf-like nanosheets and **d** coralloid and hierarchical Co_3O_4

Figure 4a shows the CV curves of the coralloid and hierarchical Co_3O_4. The measurements were performed in a potential range of −0.2 to +0.4 V (versus SCE) in 3 M KOH electrolyte at different scan rates of 10, 25, 50, and 100 mV s^{-1}. There are one pair redox peaks in the curves, indicating that coralloid and hierarchical Co_3O_4 possess a typical pseudocapacitor characteristic, which are different to the CV of $Co(OH)_2$ (Supplementary Fig. S2). The corresponding redox reactions can be expressed as follows [33–35]:

$$Co_3O_4 + OH^{-1} + H_2O \rightarrow 3CoOOH + e^{-1} \quad (4)$$

$$CoOOH + OH^{-1} \rightarrow CoO_2 + H_2O + e^{-1} \quad (5)$$

GCD curves of the coralloid and hierarchical Co_3O_4 were investigated at various current densities (0.5, 1, 2, 3, and 4 A g^{-1}) with voltage between −0.2 and 0.4 V, as shown in Fig. 4b. The specific capacitances are obtained from Eq. (1). According to the results, the specific capacitances of the coralloid and hierarchical Co_3O_4 are 591, 383, 143, 78, and 59 F g^{-1} at 0.5, 1, 2, 3, and 4 A g^{-1}, respectively. In the previous research [36, 37], the specific capacitances of the pure Co_3O_4 electrodes were only 340 and 191.2 F g^{-1} at 1 A g^{-1}, respectively. The obtained specific capacitance is higher than the previous research, which is attributed to the coralloid and hierarchical nanostructures.

Electrical impedance spectroscopy measurements were also carried out for the materials, as shown in Fig. 4c. Clearly, the Nyquist plots before and after 100 cycles are composed of a semicircle profile at the high-frequency region and a straight line tendency at the low-frequency region. The semicircle in the high-frequency range is attributed to the three sections, including electrolyte, electroactive material, and the contact resistance between the electroactive material and the current collector. And, the straight line is related to the diffusive resistance. There is no obvious difference in the high-frequency range on the 1st and 100th cycles demonstrating that the Co_3O_4 electrode is suitable for supercapacitors.

For supercapacitors, cycling stability is another very important parameter. Therefore, galvanostatic charge–discharge measurements of the coralloid and hierarchical Co_3O_4 nanostructures for 2000 cycles are further conducted at a current density of 1 A g^{-1}, as shown in Fig. 4d. The result shows that there is almost no decrease and the capacitance still remains about 97 % after 2000 cycles, indicating their excellent electrochemical stability. Compared to previous research [26, 36, 38, 39], the as-prepared coralloid and hierarchical Co_3O_4 exhibit superior electrochemical stability.

The BET measurement was performed to investigate the surface area and pore-size distribution of the obtained coralloid and hierarchical Co_3O_4 and $Co(OH)_2$ precursor. Figure 5a, b shows that the BET surface area of $Co(OH)_2$ precursor is 22.54 m^2 g^{-1}, and the BJH pore size distribution of the average pore width is about 6.98 nm, respectively. After calcinations, the BET surface area of the Co_3O_4 is 34.95 m^2 g^{-1} and the pore-size distribution centered at 5.75 nm, as shown in Fig. 5c, d. The BET surface area of Co_3O_4 is not large, so the supercapacitor may not be concerned with the surface area. We believe that the good supercapacitor performances in our research could be ascribed to the remarkable unique coralloid and hierarchical Co_3O_4 nanostructures with a favorable feature, which not only act as both active devices and interconnects but also short diffusion path lengths to electrons and ions, leading to the high specific capacitance and long cycling stability.

Conclusions

In summary, coralloid and hierarchical Co_3O_4 nanostructures were successfully prepared through a two-step route of room temperature solution-phase process and subsequent calcination. The as-prepared Co_3O_4 possessed a high specific capacitance and still remained 97 % after 2000 cycles. All the data showed that the coralloid and hierarchical Co_3O_4 nanostructures can be suitable for electrochemical supercapacitor devices. This method offers a simple, economical, and convenient way to obtain high supercapacitor performance Co_3O_4 nanostructure, which will have greatly industrial application in supercapacitor.

Acknowledgments The financial support from the Natural Science Foundation of China (No. 21301007) and the Hong Kong Polytechnic University (No. G-UC35) is acknowledged.

References

1. Rai AK, Gim J, Trang Vu T, Ahn D, Cho SJ, Kim J (2014) High rate capability and long cycle stability of $Co_3O_4/CoFe_2O_4$ nanocomposite as an anode material for high-performance secondary lithium ion batteries. J Phys Chem C 118(21):11234–11243
2. Liu WW, Li X, Zhu MH, He X (2015) High-performance all-solid state asymmetric supercapacitor based on Co_3O_4 nanowires and carbon aerogel. J Power Sources 282:179–186
3. Ke QQ, Tang CH, Yang ZC, Zheng MR, Mao L, Liu HJ, Wang J (2015) 3D nanostructure of carbon nanotubes decorated Co_3O_4 nanowire arrays for high performance supercapacitor electrode. Electrochim Acta 163:9–15
4. Balasubramanian S, Kamaraj PK (2015) Fabrication of natural polymer assisted mesoporous Co_3O_4/carbon composites for supercapacitors. Electrochim Acta 168:50–58
5. Salunkhe RR, Kamachi Y, Torad NL, Hwang SM, Sun Z, Dou SX, Kim JH, Yamauchi Y (2014) Fabrication of symmetric supercapacitors based on MOF-derived nanoporous carbons. J Mater Chem A 2(46):19848–19854
6. Salunkhe RR, Lee Y-H, Chang K-H, Li J-M, Simon P, Tang J, Torad NL, Hu C-C, Yamauchi Y (2014) Nanoarchitectured graphene-based supercapacitors for next-generation energy-storage applications. Chem-a Eur J 20(43):13838–13852
7. Torad NL, Salunkhe RR, Li Y, Hamoudi H, Imura M, Sakka Y, Hu C-C, Yamauchi Y (2014) Electric double-layer capacitors based on

highly graphitized nanoporous carbons derived from ZIF-67. Chem-a Eur J 20(26):7895–7900
8. Wang Y, Lei Y, Li J, Gu L, Yuan H, Xiao D (2014) Synthesis of 3D-nanonet hollow structured Co_3O_4 for high capacity supercapacitor. ACS Appl Mater Interfaces 6(9):6739–6747
9. Deori K, Ujjain SK, Sharma RK, Deka S (2013) Morphology controlled synthesis of nanoporous Co_3O_4 nanostructures and their charge storage characteristics in supercapacitors. ACS Appl Mater Interfaces 5(21):10665–10672
10. Zhong J-H, Wang A-L, Li G-R, Wang J-W, Ou Y-N, Tong Y-X (2012) Co_3O_4/Ni(OH)(2) composite mesoporous nanosheet networks as a promising electrode for supercapacitor applications. J Mater Chem 22(12):5656–5665
11. Ramadoss A, Kim SJ (2014) Enhanced supercapacitor performance using hierarchical TiO2 nanorod/Co(OH)2 nanowall array electrodes. Electrochim Acta 136:105–111
12. Xu G-L, Li J-T, Huang L, Lin W, Sun S-G (2013) Synthesis of Co_3O_4 nano-octahedra enclosed by {111} facets and their excellent lithium storage properties as anode material of lithium ion batteries. Nano Energy 2(3):394–402
13. Xu J, Gao P, Zhao TS (2012) Non-precious Co_3O_4 nano-rod electrocatalyst for oxygen reduction reaction in anion-exchange membrane fuel cells. Energy Environ Sci 5(1):5333–5339
14. Ali GAM, Fouad OA, Makhlouf SA, Yusoff MM, Chong KF (2014) Co_3O_4/SiO_2 nanocomposites for supercapacitor application. J Solid State Electrochem 18(9):2505–2512
15. Xia X, Tu J, Zhang Y, Wang X, Gu C, X-b Z, Fan HJ (2012) High-quality metal oxide core/shell nanowire arrays on conductive substrates for electrochemical energy storage. ACS Nano 6(6):5531–5538
16. Rakhi RB, Chen W, Hedhili MN, Cha D, Alshareef HN (2014) Enhanced rate performance of mesoporous Co_3O_4 nanosheet supercapacitor electrodes by hydrous RuO_2 nanoparticle decoration. ACS Appl Mater Interfaces 6(6):4196–4206
17. Zhang JJ, Huang T, Yu AS (2015) Synthesis and effect of electrode heat-treatment on the superior lithium storage performance of Co_3O_4 nanoparticles. J Power Sources 273:894–903
18. Sun H, Liu Y, Yu Y, Ahmad M, Nan D, Zhu J (2014) Mesoporous Co_3O_4 nanosheets-3D graphene networks hybrid materials for high-performance lithium ion batteries. Electrochim Acta 118:1–9
19. Han L, Tang P, Zhang L (2014) Hierarchical Co_3O_4@PPy@MnO_2 core-shell-shell nanowire arrays for enhanced electrochemical energy storage. Nano Energy 7:42–51
20. Zhang G, Wang T, Yu X, Zhang H, Duan H, Lu B (2013) Nanoforest of hierarchical Co_3O_4@$NiCo_2O_4$ nanowire arrays for high-performance supercapacitors. Nano Energy 2(5):586–594
21. Wen Z, Zhu L, Li Y, Zhang Z, Ye Z (2014) Mesoporous Co_3O_4 nanoneedle arrays for high-performance gas sensor. Sensors Actuators B Chem 203:873–879. doi:10.1016/j.snb.2014.06.124
22. Padmanathan N, Selladurai S, Razeeb KM (2015) Ultra-fast rate capability of a symmetric supercapacitor with a hierarchical Co_3O_4 nanowire/nanoflower hybrid structure in non-aqueous electrolyte. Rsc Adv 5(17):12700–12709
23. Zhang X, Zhao Y, Xu C (2014) Surfactant dependent self-organization of Co_3O_4 nanowires on Ni foam for high performance supercapacitors: from nanowire microspheres to nanowire paddy fields. Nanoscale 6(7):3638–3646
24. Cai D, Huang H, Wang D, Liu B, Wang L, Liu Y, Li Q, Wang T (2014) High-performance supercapacitor electrode based on the unique ZnO@Co_3O_4 core/shell heterostructures on nickel foam. ACS Appl Mater Interfaces 6(18):15905–15912
25. Singh AK, Sarkar D, Khan GG, Mandal K (2014) Designing one dimensional Co-Ni/Co3O4-NiO core/shell nano-heterostructure electrodes for high-performance pseudocapacitor. Appl Phys Lett 104 (13)
26. Wang B, Zhu T, Wu HB, Xu R, Chen JS, Lou XW (2012) Porous Co_3O_4 nanowires derived from long Co(CO3)(0.5)(OH)center dot 0.11H(2)O nanowires with improved supercapacitive properties. Nanoscale 4(6):2145–2149
27. Mahmoud WE, Al-Agel FA (2011) A novel strategy to synthesize cobalt hydroxide and Co_3O_4 nanowires. J Phys Chem Solids 72(7):904–907
28. Dong Q, Kumada N, Yonesaki Y, Takei T, Kinomura N (2011) Cobalt oxide (Co_3O_4) nanorings prepared from hexagonal beta-Co(OH)(2) nanosheets. Mater Res Bull 46(8):1156–1162
29. Xu J, Gao L, Cao J, Wang W, Chen Z (2010) Preparation and electrochemical capacitance of cobalt oxide (Co_3O_4) nanotubes as supercapacitor material. Electrochim Acta 56(2):732–736
30. Wang X, Ding J, Yao S, Wu X, Feng Q, Wang Z, Geng B (2014) High supercapacitor and adsorption behaviors of flower-like MoS2 nanostructures. J Mater Chem A 2(38):15958–15963
31. Zhu T, Chen JS, Lou XW (2010) Shape-controlled synthesis of porous Co_3O_4 nanostructures for application in supercapacitors. J Mater Chem 20(33):7015–7020
32. Hou L, Yuan C, Yang L, Shen L, Zhang F, Zhang X (2011) Urchin-like Co_3O_4 microspherical hierarchical superstructures constructed by one-dimension nanowires toward electrochemical capacitors. Rsc Adv 1(8):1521–1526
33. Wu JB, Lin Y, Xia XH, Xu JY, Shi QY (2011) Pseudocapacitive properties of electrodeposited porous nanowall Co_3O_4 film. Electrochim Acta 56(20):7163–7170
34. X-h X, J-p T, Y-j M, Wang X-l, C-d G, X-b Z (2011) Self-supported hydrothermal synthesized hollow Co_3O_4 nanowire arrays with high supercapacitor capacitance. J Mater Chem 21(25):9319–9325
35. Wang H-W, Hu Z-A, Chang Y-Q, Chen Y-L, Zhang Z-Y, Yang Y-Y, Wu H-Y (2011) Preparation of reduced graphene oxide/cobalt oxide composites and their enhanced capacitive behaviors by homogeneous incorporation of reduced graphene oxide sheets in cobalt oxide matrix. Mater Chem Phys 130(1–2):672–679
36. Deng J, Kang L, Bai G, Li Y, Li P, Liu X, Yang Y, Gao F, Liang W (2014) Solution combustion synthesis of cobalt oxides (Co_3O_4 and Co_3O_4/CoO) nanoparticles as supercapacitor electrode materials. Electrochim Acta 132:127–135
37. Liu W, Xu L, Jiang D, Qian J, Liu Q, Yang X, Wang K (2014) Reactable ionic liquid assisted preparation of porous Co_3O_4 nanostructures with enhanced supercapacitive performance. CrystEngComm 16(12):2395–2403
38. Wang X, Yao S, Wu X, Shi Z, Sun H, Que R (2015) High gas-sensor and supercapacitor performance of porous Co_3O_4ultrathin nanosheets. RSC Adv 5(23):17938–17944
39. Tummala R, Guduru RK, Mohanty PS (2012) Nanostructured Co_3O_4 electrodes for supercapacitor applications from plasma spray technique. J Power Sources 209:44–51